Transport Properties of Lennard-Jones Mixtures: A Molecular Dynamics Simulation Study

Song Hi Lee

Department of Chemistry, Kyungsung University, Busan 608-736, Korea. E-mail: shlee@ks.ac.kr
Received February 14, 2008

Equilibrium molecular dynamics simulations in a canonical ensemble are performed to evaluate the transport coefficients of several Lennard-Jones (LJ) mixtures at a liquid argon states of 94.4 K and 1 atm via modified Green-Kubo formulas. Two component mixture of A and B is built by considering the interaction between A and A as the attractive (*A*) potential, that between A and B as the attractive potential (*A*), and that between B and B as the repulsive potential (*R*), labelled as *AAR* mixture. Three more mixtures - *ARA*, *ARR*, and *RAR* are created in the same way. The behavior of the LJ energy and the transport properties for all the mixtures is easily understood in terms of the portion of attractive potential (*A* %). The behavior of the thermal conductivities by the translational energy transport due to molecular motion exactly coincides with that of diffusion constant while that of the thermal conductivities by the potential energy transport due to molecular motion is easily understood from the fact that the LJ energy of *AAR*, *ARR*, and *RAR* mixtures increases negatively with the increase of *A* % from that of the pure repulsive system while that of *ARA* changes rarely.

Key Words : Diffusion, Shear viscosity, Thermal conductivity, Lennard-Jones mixtures, Molecular dynamics simulation

Introduction

Two-component fluids can undergo segregation or phase separation[1] which is akin to that in binary clusters.[2-5] While some gross features of the late-stage of the demixing process have their bulk phase analogs, the dynamics is strongly influenced by fluctuations and other finite size effects. The morphology of the segregated fluids arises from an often delicate balance of internal and surface force as well as entropic contributions. The interfaces separating stable phases may have thickness that are comparable to the fluid dimensions, and strong particle correlations may exist within the fluid as a result of surface forces.[2,3]

The first computer simulation study for the equation of state of an equimolar binary mixture of nearly equal hard spheres was carried out by Rotenberg in the 1960s using Monte Carlo method.[6] An extensive series of computations for Lennard-Jones mixtures followed in the 1970s to determine the excess thermodynamic functions of mixing.[7,8] After that, a number of molecular dynamics studies on the transport coefficients in binary fluid mixtures have been reported.[9-11] There was good agreement among these studies, and therefore it can be said that the basic method to calculate the transport coefficients by MD simulations has been established.

Transport coefficients - self-diffusion coefficient, D, shear viscosity, η, and thermal conductivity, λ - of pure fluids can be calculated from equilibrium molecular dynamics simulation by the infinite time integral of an equilibrium correlation function of the form known as the Green-Kubo formulas.[12-14] Associated with any expression of the Green-Kubo formulas there is also the Einstein formula to calculate the transport properties. In recent years, non-equilibrium molecular dynamics (NEMD) simulations have emerged as a powerful tool for the study of transport coefficients of both simple and molecular fluids.[15-17]

In the present paper, we report new results of equilibrium molecular dynamics (EMD) simulations of mixtures of two LJ particles in a canonical ensemble (NVT fixed). The goal of this study is to elucidate the dependence of transport properties of LJ mixtures on the mole fraction of component A, x_A. This paper is organized as follows: We present the molecular models and details of MD simulation methods in next section, theories for transport properties in Section III, our simulation results in Section IV, and concluding remarks in Section V.

Molecular Models and NVT MD Simulations

One of simpler, more idealized, pair potentials commonly used in computer simulations is a simple Lennard-Jones (LJ) 12-6 potential :

$$v^{LJ} = 4\varepsilon\left[\left(\frac{\sigma}{r}\right)^{12} - \left(\frac{\sigma}{r}\right)^{6}\right]. \quad (1)$$

Values of the LJ potential parameters of ε/k = 120 K and σ = 0.34 nm provide reasonable agreement with the experimental properties of liquid argon. This is the typical LJ potential for the attractive (*A*) potential used in this EMD simulation study with the LJ potential parameters.

It is often useful to divide more realistic potentials into separate attractive and repulsive components, and the separation proposed by Weeks *et al.*[18] involves splitting the potential at the minimum (r_m). For the LJ potential, the repulsive part is called the WCA potential:

$$v^{WCA}(r) = \begin{cases} 4\varepsilon\left[\left(\frac{\sigma}{r}\right)^{12} - \left(\frac{\sigma}{r}\right)^{6}\right] + \varepsilon, & r \le r_m = 2^{1/6}\sigma \\ 0, & r > r_m \end{cases} . \quad (2)$$

The WCA potential with the same LJ potential parameters for the attractive potential (A) is used for the repulsive (R) potential in this study.

We begin by considering mixtures of two LJ particles interacting through the above attractive (A) or repulsive (R) potential at a liquid argon state of constant temperature and volume - 94.4 K and 1.374 g/cc. For two component mixture of A and B, the interaction between A and A is chosen as the attractive (A) potential, that between A and B as the attractive potential (A), and that between B and B as the repulsive potential (R). This mixture is labelled as *AAR*. Three more mixtures - *ARA*, *ARR*, and *RAR* are created in the same way. The mole fraction of particle A, x_A, is chosen as 0.125, 0.25, 0.375, and 0.5. Accordingly the mixtures are further labelled as *AAR1*, *AAR2*, *AAR3*, *etc.*

The preliminary canonical ensemble (NVT fixed) EMD simulations for 8000 LJ particles of several mixtures were started in the cubic box of length L = 7.2826 nm, of which the density is equal to 1.374 g/cm^3 at 94.4 K and 1 atm. The inter-particle potential was truncated at 2.5 σ, which is the cutoff distance used in many other simulations. Long range corrections to the energy, pressure, *etc.* due to the potential truncation were included in these properties by assuming that the pair distribution function was uniform beyond the cutoff distance.[19] The equations of motion were solved using the velocity Verlet algorithm[20] with a time step of 10^{-14} second. The systems were fully equilibrated and the equilibrium properties were averaged over five blocks of 10,000 time steps. The configurations of LJ particles were stored every time step for further analysis.

Green-Kubo Formula

As dynamic properties, we consider diffusion constant (D), shear viscosity (η), thermal conductivity (λ), and friction constant (ζ) of LJ mixture systems. Diffusion constant can be obtained through two routes: the Green-Kubo formula from velocity auto-correlation functions (VAC):

$$D_s = \frac{1}{3}\int_0^\infty \langle \mathbf{v}_i(t)\cdot\mathbf{v}_i(0)\rangle dt . \quad (3a)$$

and the Einstein formula from mean square displacements (MSD):

$$D_s = \frac{1}{6}\lim_{t\to\infty}\frac{d<|\mathbf{r}(t)\cdot\mathbf{r}(0)|^2}{dt} . \quad (3b)$$

Shear viscosity is calculated by the modified Green-Kubo formula for better statistical accuracy[21,22]:

$$\eta = \frac{V}{kT}\int_0^\infty dt \sum_i \langle P_{i\alpha\beta}(0)\cdot P_{i\alpha\beta}(t)\rangle , \quad (4)$$

where $P_{i\alpha\beta}(t) = \frac{1}{V}\left[mv_{i\alpha}(t)\cdot v_{i\beta}(t) + \sum_{j\neq i} r_{i\alpha}(t)\cdot f_{i\beta}(t)\right]$ with $\alpha\beta$= xy, xz, yx, yz, zx, and zy.

Thermal conductivity is also calculated by the modified Green-Kubo formula for better statistical accuracy[21,22]:

$$\lambda = \frac{V}{kT^2}\int_0^\infty dt \sum_i \langle \dot{q}_{i\alpha}(0)\cdot\dot{q}_{i\alpha}(t)\rangle , \quad (5)$$

where α = x, y, and z. The heat flux by each molecule is

$$\dot{q}_{i\alpha}(0) = \frac{1}{V}\left\{\varepsilon_i(t)\cdot v_{i\alpha}(t) + \frac{1}{2}\sum_{j\neq i} r_{ij\alpha}(t)\cdot[\mathbf{v}_i(t)\cdot\mathbf{f}_{ij}(t)]\right\} . \quad (6)$$

Here, the energy of molecule i is given by

$$\varepsilon_i(t) = \frac{1}{2}m_i v_i(t)^2 + \frac{1}{2}\sum_{j\neq i}\Phi[r_{ij}(t)] . \quad (7)$$

The heat flux by each molecule, Eq. (6), with the energy of molecule, Eq. (7), consists of three contributions :

$$\dot{q}_{i\alpha} = \dot{q}^{tm}_{i\alpha} + \dot{q}^{pm}_{i\alpha} + \dot{q}^{ti}_{i\alpha}, \quad (8)$$

where

$$\dot{q}^{tm}_{i\alpha} = \frac{1}{V}\left[\frac{1}{2}m_i v_i^2\right]v_{i\alpha}, \quad (9)$$

$$\dot{q}^{pm}_{i\alpha} = \frac{1}{V}\left[\frac{1}{2}\sum_{j\neq i}\Phi(r_{ij})\right]v_{i\alpha}, \quad (10)$$

and

$$\dot{q}^{ti}_{i\alpha} = \frac{1}{V}\left[\frac{1}{2}\sum_{j\neq i} r_{ij\alpha}(\mathbf{v}_i\cdot\mathbf{f}_{ij})\right], \quad (11)$$

$\dot{q}^{tm}_{i\alpha}$ and $\dot{q}^{pm}_{i\alpha}$ are the translational and the potential energy transport, respectively, due to molecular motion and $\dot{q}^{ti}_{i\alpha}$ is the translational energy transfer due to molecular interaction. Hence, the thermal conductivity, Eq. (5), consists of three contributions:

$$\lambda_t = \lambda_{tm} + \lambda_{pm} + \lambda_{ti} . \quad (12)$$

Finally the friction constant is defined as

$$\zeta = \frac{1}{3kT}\int_0^\infty \langle \mathbf{f}_i(t)\cdot\mathbf{f}_i(0)\rangle dt . \quad (13)$$

Results and Discussion

Mixtures with the repulsive potential between components A and B, *ARA* and *ARR*, exhibit segregation as shown in Figure 1 while those with the attractive potential between A and B, *AAR* and *RAR*, are a mixed state of two LJ particles. Apparently the segregation affects the transport properties of mixtures.

Table 1 contains all the results of pure systems and several mixtures in this equilibrium molecular dynamics (EMD) simulation study of canonical (NVT) ensemble. Portion of attractive potential (A %) is defined as the number of attractive interacting pairs divided by that of the total interacting pairs. This quantity of *AAR*, *ARR*, and *RAR* mixtures increases from the pure repulsive system as the mole fraction of component A, x_A, increases but that of *ARA*

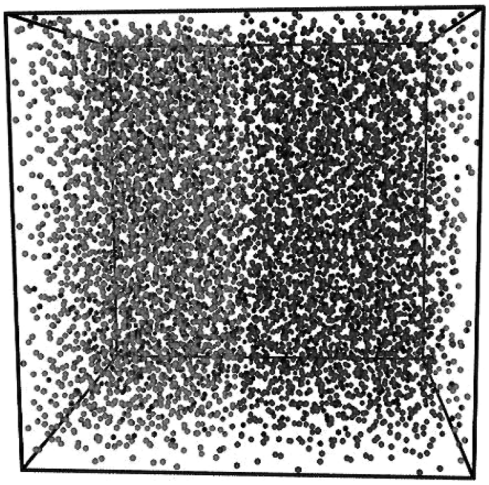

Figure 1. Snap shot of *ARA4* system at a state of 94.4 K and 1 atm.

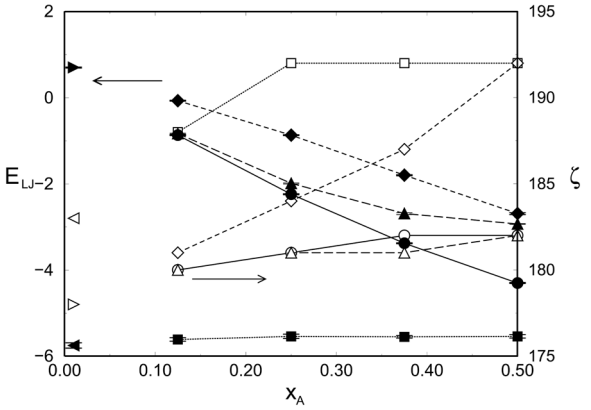

Figure 2. LJ energy (E_{LJ} in kJ/mol) and friction constant (ζ in g/mol·ps). ◀ and ▶: LJ energy of the pure attractive and the pure repulsive systems, ●: *AAR* mixture, ■: *ARA* mixture, ◆: *ARR* mixture, and ▲: *RAR* mixture. The corresponding white symbols are for the friction constant. The error bars represent the uncertainties in the last reported digit(s) given in parenthesis of Table 1.

mixture decreases from the pure attractive system. The dependence of the transport properties of several mixtures on the mole fraction of component A, x_A, is easily understood by this quantity in the below.

We plot the LJ energy and the friction constant in Figure 2. The LJ energy of all the mixtures lies between those of the pure attractive (*A*) and the pure repulsive (*R*) systems. As the mole fraction of component A, x_A, increases, the LJ energy of *AAR*, *ARR*, and *RAR* increases negatively with the increase of portion of attractive potential (*A* %) from that of the pure repulsive system while that of *ARA* changes rarely since this mixture consists of two separate attractive systems. For ideal liquid mixtures, one would expect that each of the properties would depend linearly on composition, i.e.,

$$Y = x_A Y_A + (1 - x_A) Y_B, \tag{14}$$

where *Y* is a property. The behavior of the LJ energy of *ARR* shows a perfect linear model since this mixture consists of one attractive system surrounded by repulsive particles and the *A* % increases linearly with x_A. On the other hand, the behavior of the LJ energy of *AAR* and *RAR* does not show a perfect linear model but it seems close to an exponential model, given by

$$Y = \exp[x_A \ln Y_A + (1 - x_A) \ln Y_B]. \tag{15}$$

This model is an engineering correlation recommended for

Table 1. Portion of attractive potential (*A* %), LJ energy (E_{LJ} in kJ/mol), diffusion constant (D(VAC) in 10^{-5} cm^2/sec, Eq. (3a)), shear viscosity (η in mp, Eq. (4)), thermal conductivities (λ in 10^{-4} cal/K·cm·sec), and friction constant (ζ in g/(ps·mol), Eq. (13)) of mixtures of LJ particles at T = 94.4 K and p = 1 atm. Uncertainties in the last reported digit(s) are given in parenthesis

System	*A* %	$-E_{LJ}$	D(VAC)	η	λ_{tm}	λ_{pm}	λ_{ti}	λ_t (Eq. 12)	ζ
Pure *A*	100	5.75(6)	2.45(5)	3.25(4)	0.143(2)	0.892(25)	0.852(29)	1.887	183(0)
Pure *R*	0	−0.70(1)	3.09(6)	2.69(2)	0.167(2)	0.021(1)	1.549(32)	1.737	178(1)
AAR1	23.4	0.87(1)	2.89(2)	3.42(3)	0.163(1)	0.128(2)	1.134(12)	1.425	180(0)
AAR2	43.8	2.24(1)	2.73(4)	3.59(3)	0.154(1)	0.264(6)	0.805(13)	1.223	181(0)
AAR3	60.9	3.38(1)	2.62(5)	3.40(5)	0.152(2)	0.420(11)	0.577(8)	1.149	182(0)
AAR4	75.0	4.30(1)	2.47(3)	2.90(3)	0.143(1)	0.551(9)	0.413(5)	1.107	182(0)
ARA1	78.1	5.61(4)	2.35(2)	3.18(7)	0.140(2)	0.794(7)	0.733(11)	1.667	188(0)
ARA2	62.5	5.54(5)	2.27(4)	3.13(3)	0.134(3)	0.718(14)	0.607(11)	1.459	192(0)
ARA3	53.1	5.55(3)	2.21(2)	2.57(4)	0.132(3)	0.700(8)	0.505(11)	1.337	192(1)
ARA4	50.0	5.54(4)	2.25(5)	1.92(4)	0.133(4)	0.712(13)	0.401(2)	1.246	192(0)
ARR1	1.6	0.07(1)	2.98(5)	2.31(2)	0.164(3)	0.051(2)	1.250(34)	1.465	181(0)
ARR2	6.3	0.87(1)	2.94(4)	1.90(4)	0.164(2)	0.095(2)	1.025(19)	1.284	184(0)
ARR3	14.1	1.80(1)	2.92(4)	1.40(1)	0.163(2)	0.144(5)	0.779(11)	1.086	187(1)
ARR4	25.0	2.69(2)	2.78(4)	1.01(1)	0.156(2)	0.187(4)	0.558(7)	0.901	192(0)
RAR1	21.9	0.83(1)	2.91(2)	3.44(5)	0.161(1)	0.110(1)	1.131(17)	1.402	180(0)
RAR2	37.5	1.99(1)	2.63(5)	3.51(2)	0.151(3)	0.176(2)	0.797(13)	1.124	181(0)
RAR3	46.9	2.69(2)	2.51(5)	3.26(2)	0.145(3)	0.228(4)	0.560(11)	0.933	181(0)
RAR4	50.0	2.93(1)	2.48(5)	2.80(5)	0.144(2)	0.241(5)	0.410(6)	0.795	182(1)

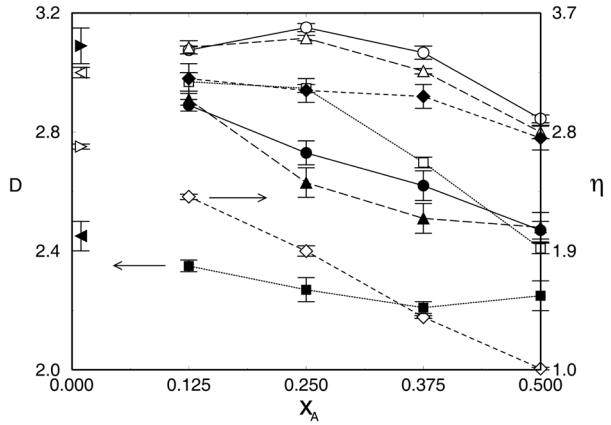

Figure 3. Diffusion constant (D in 10^{-5} cm^2/sec: the black symbols) and shear viscosity (η in mp: the white symbols) as a function of the mole fraction of component A, x_A, at a state of 94.4 K and 1 atm obtained in this NVT-EMD simulation study. The legends are the same as in Fig. 2.

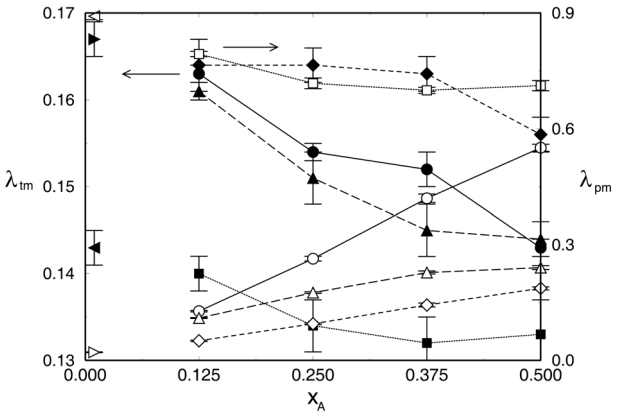

Figure 4. Thermal conductivities (in 10^{-4} cal/K·cm·sec, λ_{tm}: the black symbols and λ_{pm}: the white symbols) as a function of the mole fraction of component A, x_A, at a state of 94.4 K and 1 atm obtained in this NVT-EMD simulation study. The legends are the same as in Fig. 2.

predicting liquid mixtures in the absence of mixture property data.

The friction constant increases generally with the increase of the mole fraction of A, x_A. The trend of the friction constant of *AAR*, *ARR*, and *RAR*, which increases with the increase of *A* % from that of the pure repulsive system, is similar to that of the LJ energy. Note that the behavior of the friction constant of *AAR* and *RAR* is almost equal each other since these mixtures are a mixed state of two LJ particles and the *A* % increases by almost equal amount with the increase of the mole fraction of A, x_A. The behavior of the friction constant of *AAR*, *ARR*, and *RAR* shows a linear model generally.

In Figure 3, we plot diffusion constant and viscosity for pure systems and several mixtures as a function of x_A, which were obtained through the Green-Kubo formulas (Eqs. 3(a) and (4)) in this EMD simulation study in NVT ensemble. The calculated diffusion coefficient and shear viscosity for the pure attractive system at a state of 94.4 K and 1 atm are close to the experimental measures ($D = 2.43 \times 10^{-5}$ cm^2/sec at 90 K and 1.374 g/cm^3, and $\eta = 1.97$ mp at 94.4 K and 1 atm for pure Ar). The diffusion constant for the pure repulsive system is larger than that for the pure attractive system and the viscosity is opposite as expected. As the mole fraction of component A, x_A, increases, the diffusion constant of *AAR*, *ARR*, and *RAR* decreases with the increase of *A* % from that of the pure repulsive system, but that of *ARA* decreases with the decrease of *A* % from that of the pure attractive system since this mixture consists of two separate attractive systems which repel each other. The decreasing trend of the diffusion constant of *AAR*, *ARR*, and *RAR* with the increase of *A* % from that of the pure repulsive system is similar to the negative increase of the LJ energy and the increase of the friction constant. Here the similarity of the behavior of the diffusion constant of *AAR* and *RAR* is notable again.

The viscosity of *AAR* and *RAR* shows a similar behavior each other like the diffusion constant of those mixtures, but it increases and then decreases with the increase of *A* % from that of the pure attractive system. It is expected that mixing of attractive and repulsive particles enhances the stress of the particles to the wall larger than that of the pure attractive system and then diminishes it over about 50% of *A* %. For the case of *ARA* mixture, the viscosity decreases with the decrease of *A* % from that of the pure attractive system, but for the *ARR* mixture, the opposite is observed and the viscosity decreases almost linearly with the mole fraction of component A, x_A, from that of the pure repulsive system.

In Figures 4 and 5, we plot three thermal conductivities (λ_{tm}, λ_{pm}, and λ_{ti}) and their sum (λ_t) for pure systems and several mixtures. The experimental thermal conductivity is $\lambda_t = 2.74 \times 10^{-4}$ cal/Kcmsec at a state of 94.4 K and 1 atm for pure Ar, which is close to that of the pure attractive system in this NVT-EMD simulation study. Switching from attractive potential to repulsive potential causes to increase λ_{tm} and λ_{ti} but to decrease λ_{pm} and the total thermal conductivity, λ_t, since the decrement of λ_{pm} overcomes the

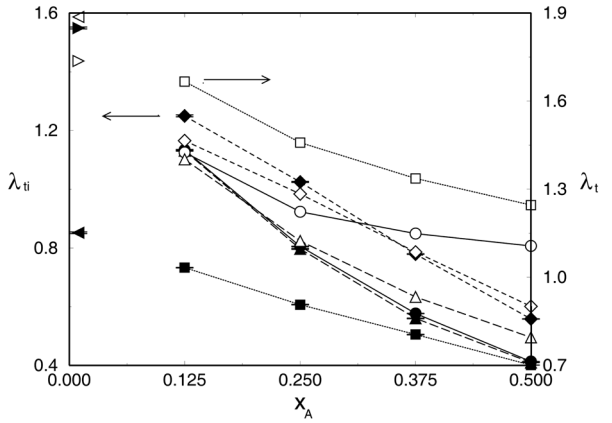

Figure 5. Thermal conductivities (in 10^{-4} cal/K·cm·sec, λ_{ti}: the black symbols and λ_t: the white symbols) as a function of the mole fraction of component A, x_A, at a state of 94.4 K and 1 atm obtained in this NVT-EMD simulation study. The legends are the same as in Fig. 2.

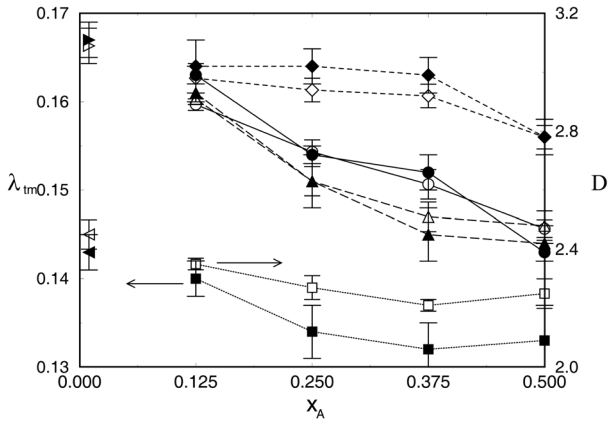

Figure 6. Comparison of λ_{tm} (in 10^{-4} cal/K·cm·sec: the black symbols) and D (in 10^{-5} cm^2/sec: the white symbols) as a function of the mole fraction of component A, x_A, at a state of 94.4 K and 1 atm obtained in this NVT-EMD simulation study. The legends are the same as in Fig. 2.

increment of λ_{tm} and λ_{ti}.

Energy transported via molecular motion governs heat conduction in gases, while energy transfer between molecules due to molecular interaction is a dominant factor in heat conduction in liquids. Liquid molecules transport energy by molecular motion and transfer their energy to other molecules by molecular interaction. Accordingly, λ_{tm} and λ_{pm} are the thermal conductivities by the translational and the potential energy transport, respectively, due to molecular motion, and λ_{ti} is that by the translational energy transfer due to molecular interaction. In general, as the mole fraction of component A, x_A, increases, λ_{tm} and λ_{ti} of all the mixtures decrease while λ_{pm} increases and as a result the sum of these three thermal conductivities decreases.

λ_{tm} of *AAR*, *ARR*, and *RAR* mixtures decrease with the increase of *A* % from that of the pure repulsive system to that of the pure attractive system while that of *ARA* mixture decreases with the decrease of *A* % from that of the pure attractive system. Since λ_{tm} is the thermal conductivity by the translational energy transport due to molecular motion, the behavior of λ_{tm} for all the mixtures exactly coincides with that of diffusion constant, D, as shown in Figure 3. In Figure 6, we compared the behaviors of D and λ_{tm} as a function of the mole fraction of component A, x_A, for all the mixtures.

It is also interesting that λ_{pm} of *AAR*, *ARR*, and *RAR* mixtures increase almost linearly with the increase of *A* % from that of the pure repulsive system while that of *ARA* mixture decrease with the decrease of *A* % from that of the pure attractive system. This is easily understood from the fact that λ_{pm} is the thermal conductivity by the potential energy transport due to molecular motion and the LJ energy of *AAR*, *ARR*, and *RAR* mixtures increases negatively with the increase of *A* % from that of the pure repulsive system while that of *ARA* changes rarely as shown in Figure 2.

λ_{ti} of *AAR*, *ARR*, and *RAR* mixtures decrease with the increase of *A* % from that of the pure repulsive system while that of *ARA* mixture decreases with the decrease of *A* % from that of the pure attractive system. The behavior of λ_{ti} for all the mixtures is very similar to that of λ_{tm}. The translational energy transfer due to molecular interaction, Eq. (11), involved with two terms - velocity and interatomic force, which are not easily analyzed. It may be only deduced that the translational energy flux due to molecular motion, Eq. (9), is involved with the velocity and that the interatomic force for *AAR*, *ARR*, and *RAR* mixtures decrease with the increase of *A* % from that of the pure repulsive system while that of *ARA* mixture decreases with the decrease of *A* % from that of the pure attractive system. The linear decrease of λ_{ti} for *ARA* and *ARR* mixtures is notable.

The sum of three thermal conductivities, λ_t, also shows a similar behavior to λ_{tm} and λ_{ti}. λ_t of *AAR*, *ARR*, and *RAR* mixtures decrease with the increase of *A* % from that of the pure repulsive system while that of *ARA* mixture decreases with the decrease of *A* % from that of the pure attractive system.

Conclusion

We present new results for transport properties of mixtures of two LJ particles at a liquid argon state of 94.4 K and 1 atm by equilibrium molecular dynamics (EMD) simulations of canonical (NVT) ensemble using modified Green-Kubo formulas. The mixtures are built by considering mixtures of two LJ particles interacting through the above attractive (*A*) or repulsive (*R*) potential. For two component mixture of A and B, the interaction between A and A is chosen as the attractive (*A*) potential, that between A and B as the attractive potential (*A*), and that between B and B as the repulsive potential (*R*). This mixture is labelled as *AAR*. Three more mixtures - *ARA*, *ARR*, and *RAR* are created in the same way.

The Lennard-Jones (LJ) energy of *AAR*, *ARR*, and *RAR* increases negatively with the increase of portion of attractive potential (*A* %) from that of the pure repulsive system while that of *ARA* changes rarely. The friction constant increases generally with the increase of the mole fraction of A, x_A. The trend of the friction constant of *AAR*, *ARR*, and *RAR*, is similar to that of the LJ energy. The diffusion constant of *AAR*, *ARR*, and *RAR* decreases with the increase of *A* % from that of the pure repulsive system, but that of *ARA* decreases with the decrease of *A* % from that of the pure attractive system. The viscosity of *AAR* and *RAR* increases and then decreases with the increase of *A* % from that of the pure attractive system. For the case of *ARA* mixture, the viscosity decreases with the decrease of *A* % from that of the pure attractive system, but for the *ARR* mixture, the opposite is observed and the viscosity decreases almost linearly with the mole fraction of component A, x_A, from that of the pure repulsive system.

The behavior of the thermal conductivities for all the mixtures by the translational energy transport due to molecular motion, λ_{tm}, exactly coincides with that of diffusion constant, D, while that of the thermal conductivities for all the mixtures by the potential energy transport due to mole-

cular motion, λ_{pm}, is easily understood from the fact that the LJ energy of *AAR*, *ARR*, and *RAR* mixtures increases negatively with the increase of *A* % from that of the pure repulsive system while that of *ARA* changes rarely. The thermal conductivity, however, by the translational energy transfer due to molecular interaction, λ_{ti}, is involved with two terms - velocity and interatomic force, which are not easily analyzed. It may be only deduced that the translational energy flux due to molecular motion is involved with the velocity and that the interatomic force for *AAR*, *ARR*, and *RAR* mixtures decrease with the increase of *A* % while that of *ARA* mixture decreases with the decrease of *A* %. The sum of three thermal conductivities for all the mixtures, λ_t, decreases with the increase of the mole fraction of component A, x_A, by favor of the behavior to λ_{tm} and λ_{ti}.

Acknowledgments. This research was supported by Kyungsung University Research Grants in 2008.

References

1. Gunton, J. D.; San Miguel, M.; Sahni, P. S. *Phase Transitions and Critical Phenomena*; Domb, C.; Lebowitz, J. L., Eds.; Academic: New York, 1983; Vol. 8.
2. Clarke, A. S.; Kapral, R.; Moore, B.; Patey, G.; Wu, X.-G. *Phys. Rev. Lett.* **1993**, *70*, 3283.
3. Clarke, A. S.; Kapral, R.; Moore, B.; Patey, G.; Wu, X.-G. *Reaction Dynamics in Clusters and in the Condensed Phase*; Jortner, J., Levine, R., Pullman, B., Eds.; Kluwer: Dordrecht, 1994; p 89.
4. Garzon, I. L.; Long, X. P.; Kawai, R.; Weare, J. H. *Europhys. Lett.* **1989**, *158*, 525.
5. Ballone, P.; Andreoni, W.; Car, R.; Parrinello, M. *Phys. Rev. Lett.* **1989**, *8*, 73.
6. Rotenberg, A. *J. Chem. Phys.* **1965**, *43*, 4377.
7. Singer, J. V. L.; Singer, K. *Molec. Phys.* **1972**, *24*, 357.
8. McDonald, I. R. *Molec. Phys.* **1972**, *23*, 41.
9. Gardner, P. J.; Heyes, D. M.; Preston, S. R. *Molec. Phys.* **1991**, *73*, 141.
10. Vogelsang, R.; Hoheisel, C.; Paolini, G. V.; Cicotti, G. *Phys. Rev. A* **1987**, *36*, 3964.
11. Hafskjol, B.; Ikeshoji, T.; Ratkje, S. K. *Molec. Phys.* **1993**, *80*, 1389.
12. Ryckaert, J.-P.; Bellemans, A.; Cicotti, G.; Paolini, G. V. *Phys. Rev. A* **1989**, *39*, 259.
13. Heyes, D. M. *Phys. Rev. B* **1988**, *37*, 5677.
14. Borgelt, P.; Hoheisel, C.; Stell, G. *Phys. Rev. A* **1990**, *42*, 789.
15. Evans, D. J. *Phys. Rev. A* **1981**, *23*, 1988.
16. Evans, D. J. *Phys. Rev. A* **1986**, *34*, 1449.
17. Cummings, P. T.; Varner, T. L. *J. Chem. Phys.* **1988**, *89*, 6391.
18. Weeks, J. D.; Chandler, D.; Anderson, H. C. *J. Chem. Phys.* **1971**, *54*, 5237.
19. Allen, M. P.; Tildesley, D. J. *Computer Simulation of Liquids*; Oxford Univ. Press: Oxford, 1987; p 64.
20. Allen, M. P.; Tildesley, D. J. *Computer Simulation of Liquids*; Oxford Univ. Press: Oxford, 1987; p 81.
21. Lee, S. H. *Bull. Kor. Chem. Soc.* **2007**, *28*, 1371.
22. Min, S. H.; Son, C. M.; Lee, S. H. *Bull. Kor. Chem. Soc.* **2007**, *28*, 1689.